

# THERMAL RESIDUAL STRESS STATE IN LASER DIODE/HEATSINK JOINT SYSTEMS DEPENDING ON THE PROPERTIES OF THE HEATSINK MATERIAL. FEM ANALYSIS\*

Dariusz Kalinski<sup>1)</sup>

The paper presents the results of calculations, performed using the finite element method (FEM), which include a comparative analysis of the residual stress state induced in the GaAs laser diode/heatsink joint systems that differed from one another in the material used for the heatsink (Cu, CuC<sub>F</sub>, AlN). This analysis permitted us to test the materials examined in terms of the level and distribution of the residual stresses developed in the system during its joining operation. The calculation results show, among other things, that in the model with the CuC<sub>F</sub> composite the maximum level of the tensile stresses generated in GaAs ( $\sigma_{MAX}$ ) is about 6 times lower than that in the systems with a conventional copper heatsink

## 1. INTRODUCTION

The materials intended for the fabrication of heatsinks for semiconductor devices are required to satisfy extremely severe demands. Among other requirements, they should have a good thermal conductivity, a low thermal expansion coefficient (close to the thermal coefficient of the semiconductor material), and the ability to join with the semiconductor device without generating considerable stresses. In the technology of semiconductor lasers, heatsinks are usually made of copper [1]. Although the thermal conductivity of copper is very good (390 W/mK), its thermal expansion coefficient  $\alpha$  ( $16.8 \times 10^{-6}/K$ ) is high and mismatched to GaAs ( $\alpha = 5.5 \times 10^{-6}/K$ ), which is the basic material

---

<sup>1)</sup> Instytut Technologii Materiałów Elektronicznych, ul. Wólczyńska 133, 01-919 Warszawa, e-mail: dkalins@poczta.onet.pl

\* This paper includes the results of investigations which are presented at EUROMAT 2001 7<sup>th</sup> European Conference on Advanced Materials and Processes, Rimini, Italy, 10-14 June 2001

used for the fabrication of lasers. During the joining operation, this mismatch between the thermal expansion coefficients results in high residual stresses (thermal stresses), being induced in the system. This deteriorates in a great measure the performance of the system. The use of other heatsink materials, such as e.g. diamond ( $\alpha = 1.0 \times 10^{-6}/K$ ), makes it possible to obtain a better matching between the thermal coefficients [2]. For obvious reasons, such a design is however expensive and difficult in fabrication. Another way in which this problem has been obviated is to use an indium interlayer to join the copper heatsink to the laser diode. Indium has a high thermal expansion coefficient ( $\alpha = 30.5 \times 10^{-6}/K$ ), but it shows good plasticity thanks to which the stresses can be relaxed [3]. The thermal conductivity of indium is however poor -  $71W/mK$  and thus the indium interlayer must be thin (e.g.,  $6 \mu m$ ). Although this does not impede the other technological requirements, it is inconsistent with the stress-reduction requirement. Moreover, indium tends to creep over the GaAs surface, resulting in the laser p-n junction being short-circuited and the laser being degraded.

In view of the above remarks, it seemed worth verifying whether such materials as the  $CuC_F$  composite [4-5] (a composite reinforced with short, randomly oriented carbon fibres - 40 vol.%  $C_F$ ,  $\alpha = 6.0 \times 10^{-6}/K$ ) or AlN nitride ceramic ( $\alpha = 3.0 \times 10^{-6}/K$ ) [6] would be suitable materials for heat-sinks (Fig.1).

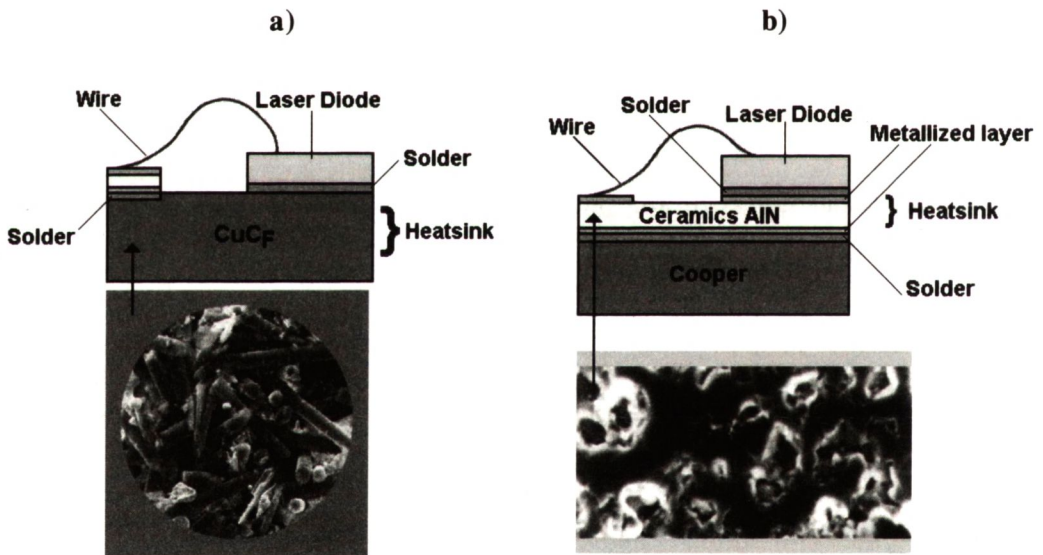


**Fig.1.** Thermal expansion coefficient ( $\alpha$ ) and thermal conductivity ( $\lambda$ ) of the materials used for heatsink: a)  $CuC_F$  composite (a composite reinforced with short, randomly oriented carbon fibres - 40 vol.%  $C_F$ ); b) AlN nitride ceramic.

## 2. SUBJECT OF THE ANALYSIS AND THE ASSUMPTIONS ADOPTED IN CALCULATING THE RESIDUAL STRESSES

The analysis used models of the laser diode/heatsink systems that differed from one another by the heatsink material (Cu,  $\text{CuC}_F$ , AlN) (Fig.2). The calculations were performed using the numerical program "LUSAS" which realised the finite element method.

The analysis of the stress state in the systems examined (plane stress state) was made based on the assumptions:

- the materials examined show isotropic properties,
- the phenomena occurring in the materials have a thermo-elasto-plastic character,
- deformations are described by the relationships defined by the linear theory of elasticity and small plastic strains,
- the plastic behaviour of the materials is described using the equations of plastic flow and adopting the Huber-Mises plasticity condition,
- no temperature gradient occurs in the materials being joined.

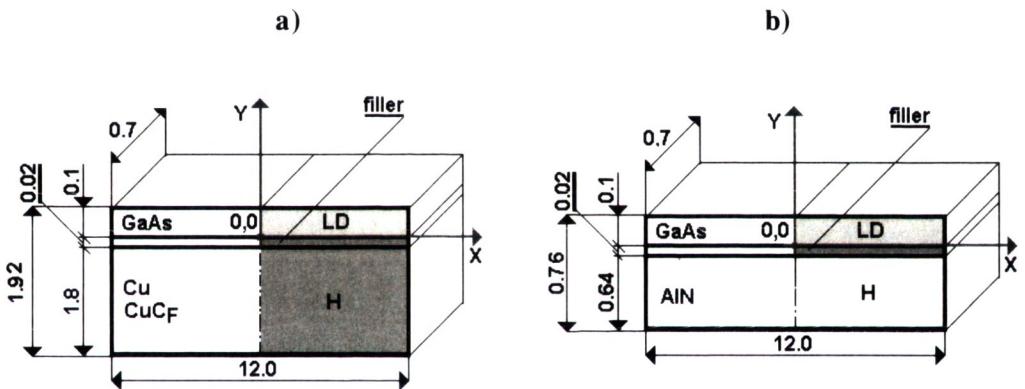


**Fig.2.** Models of the Laser Diode (LD  $\Rightarrow$  GaAs)/Heatsink (H) joint systems used in finite element calculations of thermal residual stresses: a) H  $\Rightarrow$  Cu or  $\text{CuC}_F$ , b) H  $\Rightarrow$  AlN.

Fig.3 shows an example of the finite element mesh (for a plane stress state) into which one of the models examined has been divided. The meshes were made denser in the region where, in the semiconductor element (GaAs), the stresses were expected to concentrate, i.e., at its external edge and near the semiconductor/heatsink joint line (interface). Thanks to the symmetry of the model, it was sufficient to model only one a half of the joint system.



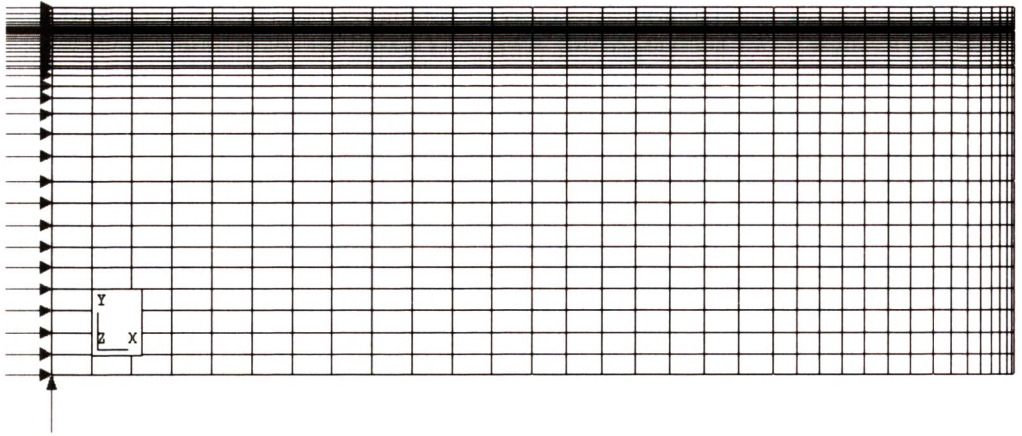


**Fig.3.** Example of the finite element mesh (GaAs/Cu or  $\text{CuC}_F$ ) used for calculating the thermal residual stresses.

The materials parameters, such as the thermal expansion coefficient  $\alpha$ , Young's modulus  $E$ , yield stress  $Re$  and the Poisson ratio  $\nu$ , used in the calculations are listed in Tab.1. The parameters were temperature - dependent, except the Poisson ratio which was assumed to be temperature - independent, and the thermal expansion coefficient and the Young modulus of the  $\text{CuC}_F$  composite since no precise data concerning the temperature variation of these parameters within the temperature range examined were available (Tab.1). The yield stress  $Re$  of the  $\text{CuC}_F$  composite was taken to be equal to that of pure copper.

**Table 1.** Materials properties (at room temperature) used for the calculation of thermal residual stresses [7-10].

Materials	$\alpha$ ( $\cdot 10^{-6}$ 1/K)	$E$ (GPa)	$Re$ (MPa)	$\nu$
Cu	16.5	131.5	50.0	0.345
$\text{CuC}_F$	(5.0-8.0)	80.8	-	0.289
AlN	4.8	310.0	-	0.289
GaAs	5.5	86.3	-	0.32
AgCu28	17.4	58.082	35.0	0.34
SnPb40	24.0	30.0	18.0	0.40
In	33.0	12.8	1.4	0.445

The load imposed on the models is associated with the laser diode/heatsink joining process. The decrease of the temperature during the period of time from the beginning of the filler metal solidification to the completion of the joining operation, together with the difference between the properties (Da, DE) of the joined materials result in residual stresses being induced in the system. It has thus been assumed that the residual stresses develop in the system during its cooling from the filler metal solidification temperature to room temperature (293 K).

In order to exaggerate the effect of the heatsink material (Cu, CuC<sub>F</sub> and AlN) on the magnitude of the generated stresses, the systems assumed in the calculations were joined with the use of a hard AgCu28 alloy. This approach was expected to support our supposition that, even under such extremely severe conditions (the solidification temperature of this alloy, at which the stresses begin to develop, is 1003 K), it is favourable to replace copper with some other material.

### 3. RESULTS AND DISCUSSION

The numerical calculations gave maps of the thermal residual stress distribution and the values of the stresses at the central region of the elements. The program employed permitted calculating the following components of the stress state: axial stress  $\sigma_y$ ,  $\sigma_x$ , tangential stress  $\sigma_{xy}$ , maximum ( $\sigma_{MAX}$ ) and minimum ( $\sigma_{MIN}$ ) principal stress.

The comparative analysis was based on the Mohr strength hypothesis, recommended for brittle materials, which assumes that the effort of the joint is determined by the highest tensile stresses ( $\sigma_{MAX}$ ) that act within the semiconductor device.

Fig.4 compares the curves of the variation of the maximum principal stress  $\sigma_{MAX}$ , and Tab.2 gives extreme magnitudes (in selected points within the semiconductor device) of the stress state components, in model GaAs/Cu (H) and GaAs/CuC<sub>F</sub> (H) systems brazed using the AgCu28 alloy.

The numerical calculation of the thermal residual stresses developed in the GaAs/heatsink (H  $\Rightarrow$  Cu, CuC<sub>F</sub>) systems show that the maximum stress  $\sigma_{MAX}$  in the semiconductor device (GaAs) occur at the free and outer wall ( $x = 6.0$  mm) of the device, at a small distance from its joint with the copper or composites heatsink (Fig.4-5a). In the GaAs/Cu joint system, maximum value of this stress is 20.0 MPa. This region of GaAs is the region of the greatest stress concentration. This means that, in the extreme case when the stress there exceeds the tensile strength of GaAs, the crack is likely to occur just in this region and that it is from there where it will propagate throughout the material.

We can infer from Fig.4, Fig.5b and Tab. 2 that the magnitude of the maximum stress  $\sigma_{MAX}$  (within the region of its maximum concentration) in a semiconductor device with the  $CuC_F$  heatsink is about 6 times lower ( $\sigma_{MAX} = 3.31$  MPa) than that in a conventional system with a copper heatsink ( $\sigma_{MAX} = 20.0$  MPa).

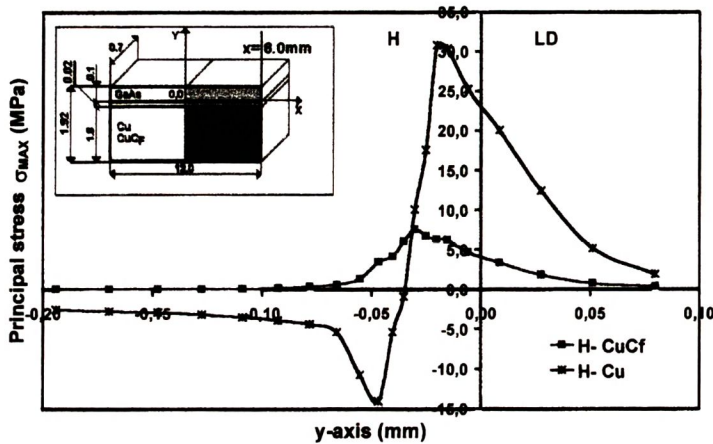


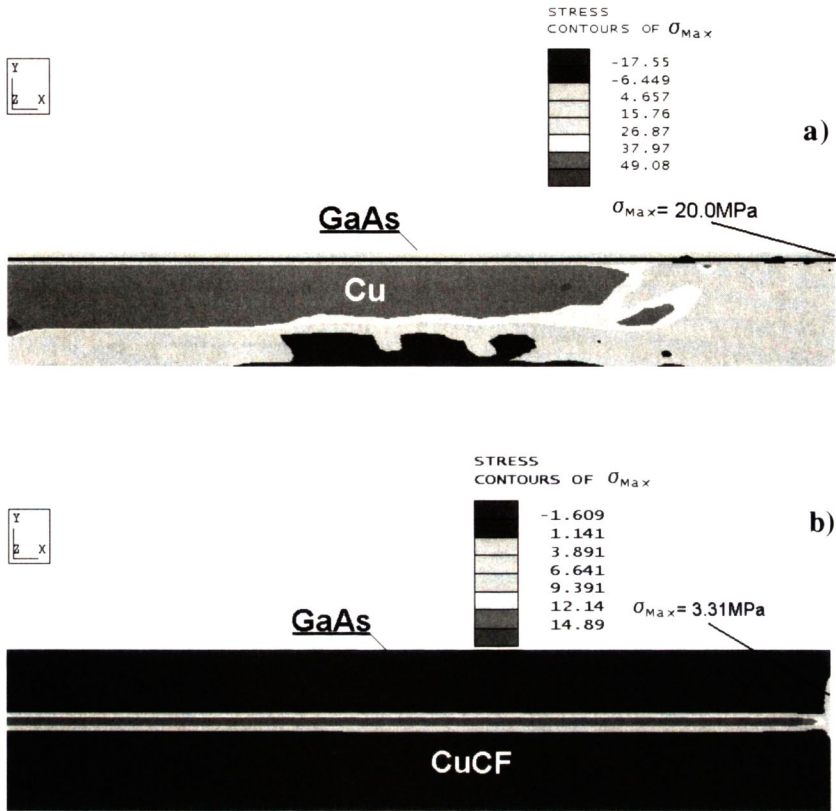
**Fig.4.** Comparison of the principal stress  $\sigma_{MAX}$  distribution along  $y$  - axis for  $x = 6.0$  in the model systems: GaAs (LD)/AgCu28/Heatsink ( $H \Rightarrow Cu, CuC_F$ ), at the maximum stress concentration region in GaAs.

**Table 2.** Calculated maximum values of the residual stresses prevailing within GaAs in the GaAs/Heatsink ( $H \Rightarrow Cu, CuC_F$ ) system joined using AgCu28 alloy.

(x;y)	Stress (MPa)									
	$\sigma_Y$		$\sigma_{MAX}$		$\sigma_X$		$\sigma_{XY}$		$\sigma_{MIN}$	
	H		H		H		H		H	
	Cu	$CuC_F$	Cu	$CuC_F$	Cu	$CuC_F$	Cu	$CuC_F$	Cu	$CuC_F$
(0.0;0.01)	-0.60	0.00	-0.44	0.00	-325.74	-4.69	-7.15	0.00	-325.87	-0.02
(0.0;0.1)	0.26	0.00	0.43	0.00	-310.56	-4.66	7.19	0.00	-310.73	-0.02
(6.0;0.01)	19.99	3.31	20.00	3.31	-1.58	-1.15	8.24	3.65	-4.55	3.14
(6.0;0.1)	1.69	0.33	1.87	0.34	0.28	0.16	-0.53	0.33	0.11	-0.03

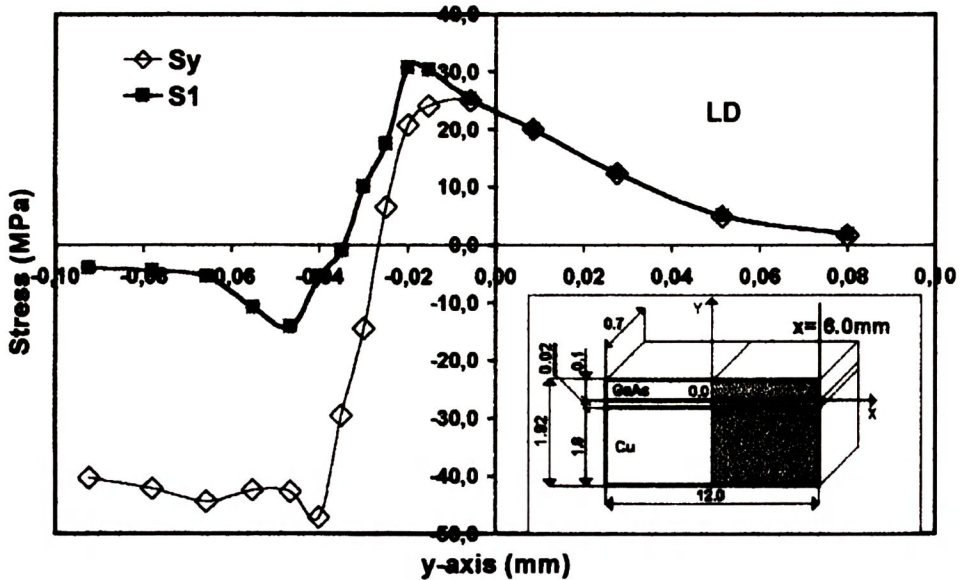
This advantageous reduction of the stress level is due, among other factors, to the decreased difference between the values of the thermal expansion coefficient of the  $CuC_F$  composite and GaAs ( $\Delta\alpha = \sim 0.5 \times 10^{-6}/K$ ) compared to the difference that occurs in a system with a copper heatsink ( $\Delta\alpha = \sim 11.3 \times 10^{-6}/K$ ).





**Fig.5.** The principal residual stress distribution ( $\sigma_{MAX}$ ) in the model bonded systems: a) GaAs/AgCu28/Cu, b) GaAs/AgCu28/CuCF.

Among all the components of the stress state in GaAs, we can distinguish the axial stress  $\sigma_y$ , since its magnitude and distribution are similar to those of the principal stress  $\sigma_{MAX}$ . This can be seen in Fig.6 where the stress  $\sigma_y$  active in the semiconductor element coincides with the principal stress  $\sigma_{MAX}$ . (When analysing the reliability of the joint, we may replace the principal stress  $\sigma_{MAX}$  by the  $\sigma_y$  component of the axial stress, which is equivalent to  $\sigma_{MAX}$ . This is particularly convenient in experimental analyses, since the component  $\sigma_y$  can be measured relatively easily and can be used for determining the effort in the sample).



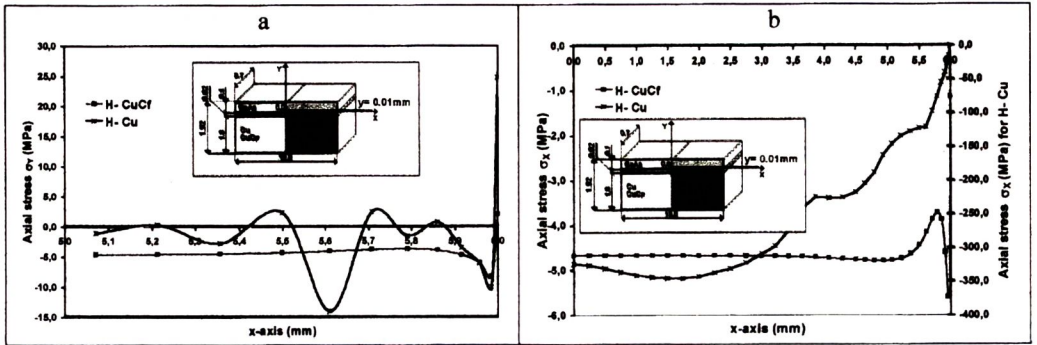
**Fig.6.** Comparison of the principal  $\sigma_{MAX}$  ( $S_1$ ) and axial  $s_y$  ( $S_y$ ) stress distribution in the model system: GaAs (LD)/AgCu28/Cu (H), along the y-axis for  $x = 6.0$ , at the maximum stress concentration region in GaAs.

Fig.7 shows the distributions of the stress  $\sigma_y$  along the x-axis within the semiconductor device of a GaAs/(Cu, CuC<sub>F</sub>) heatsink system, near the semiconductor/heatsink joint interface ( $y = 0.01$  mm). We can see that the stress active on the GaAs surface ( $x = 6.0$  mm) is tensile whereas that active inside GaAs ( $x = 0.0$  mm) - compressive. This is so because of the bending moment acting upon the semiconductor device due to the axial (along the x axis) shrinkage of the copper or composite heatsink when the system is cooled down from the joining temperature: the heatsink shrinks more than the semiconductor device. This bending moment deforms the system components after the joining process is completed. By way of example, Fig.8 shows deformation images of the models after they were cooled to a temperature of 293 K (+20°C). These deformation images show the thermal, elastic and plastic deformations that have occurred in the systems when they were cooled from 1003 K to 293 K (730°C to 20°C).

We also observe a considerable difference in the level and distribution of the axial stress  $\sigma_x$  (Fig.7b). Within the semiconductor device, the values of this stress component are negative (compression). In the copper heatsink system, the magnitude of  $s_x$  varies from about - 325.0 MPa at the central region of GaAs ( $x = 0.0$  mm,  $y = 0.01$  mm) to 0.0MPa at its outer wall GaAs ( $x = 6.0$  mm,



$y = 0.01$  mm) (Fig.7b). In the GaAs/Cu<sub>F</sub> system, the stress  $s_x$  remains almost constant and ranges from -4.5 to -6.0 MPa (Fig.7b).



**Fig.7.** Comparison of the axial stress  $\sigma_y$  (a) and  $\sigma_x$  (b) distribution along the x - axis for  $y = 0.01$  within GaAs in the model systems: GaAs/AgCu28/Cu or Cu<sub>F</sub> (H), at the region of their maximum concentration.

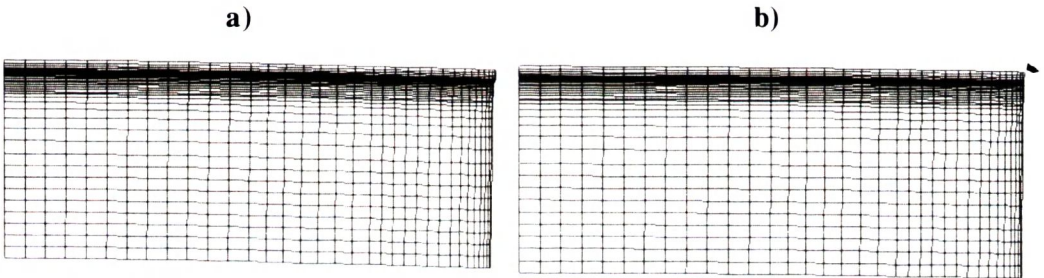


**Fig.8.** Deformation of the model LD/H bonded systems: GaAs/AgCu28/Cu (a) and GaAs/AgCu28/Cu<sub>F</sub> (b), due to a thermal load of (1003 K  $\rightarrow$  293 K).

In calculating the residual stresses in the laser diode (LD)/heatsink (H) system examined, interesting results were obtained when the heatsink was modelled of nitride ceramic AlN (Fig.1b). Tab.3 gives the extreme values of the stress state components at certain selected points inside the GaAs semiconductor device in the GaAs/AlN system. Fig.9 shows the axial distribution of the stress  $\sigma_{MAX}$  in the central region of the GaAs/AlN system ( $x = 0.0$  mm) near the GaAs - AlN interface and at its free end ( $x = 6.0$  mm).

**Table 3.** Calculated maximum values of the residual stresses prevailing within GaAs in the GaAs/AlN system joined using AgCu28 alloy.

(x,y)	Stress (MPa)				
	$\sigma_y$	$\sigma_{MAX}$	$\sigma_x$	$\sigma_{XY}$	$\sigma_{MIN}$
(0,0;0,005)	-9.90	24.86	24.83	0.87	-9.92
(0,0;0,1)	-10.01	23.07	23.04	0.87	-10.03
(6,0;0,005)	-15.88	-5.68	-18.46	11.41	-28.66
(6,0;0,1)	-10.64	-10.16	-10.23	0.183	-10.71

It should be noted that, differently from the situation with the Cu or CuC<sub>F</sub> heatsink (Fig.4), in the GaAs/AlN model, the maximum tensile stresses  $\sigma_{MAX}$  are concentrated in the central GaAs region ( $x = 0.0$  mm) at a small distance from the joint with AlN (Fig.9-10). In the central region of the system ( $x = 0.0$  mm), the stresses  $\sigma_{MAX}$  are positive (tension) across the entire thickness of the GaAs semiconductor device and their average magnitude is about 24 MPa. At the free end of the system ( $x = 6.0$  mm), the stresses  $\sigma_{MAX}$  in GaAs are negative (compression), and their magnitude ranges from - 5.68 MPa at the distance  $y = 0.005$  mm from the GaAs - AlN interface to - 10.16 MPa at  $y = 0.1$  mm.

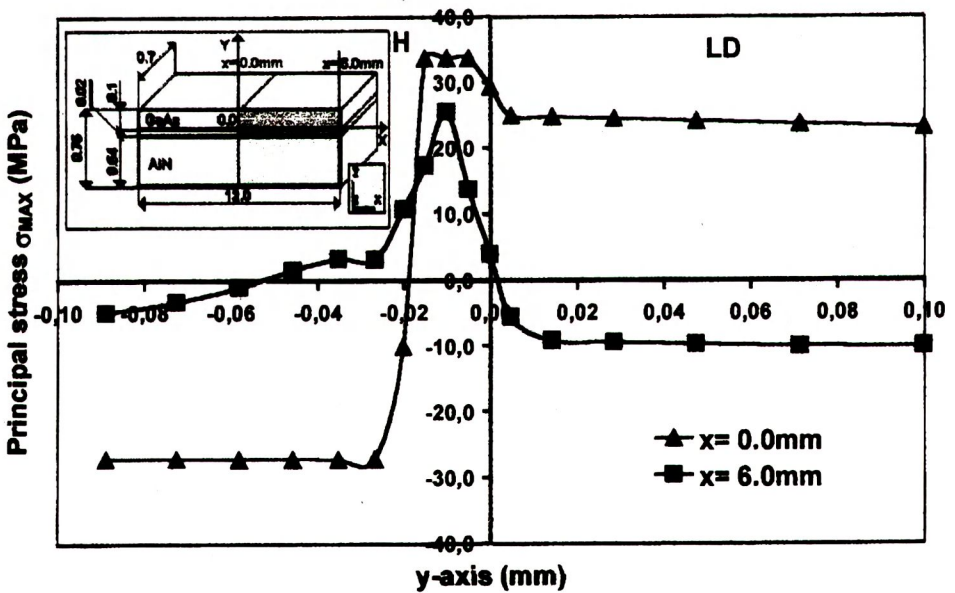


**Fig.9.** The principal stress curves  $\sigma_{MAX}$  in the model system: GaAs (LD)/AgCu28/AlN (H), along the y - axis ( $y \in -0.1,0.1$ ) at  $x = 0.0$  and  $x = 6.0$ .

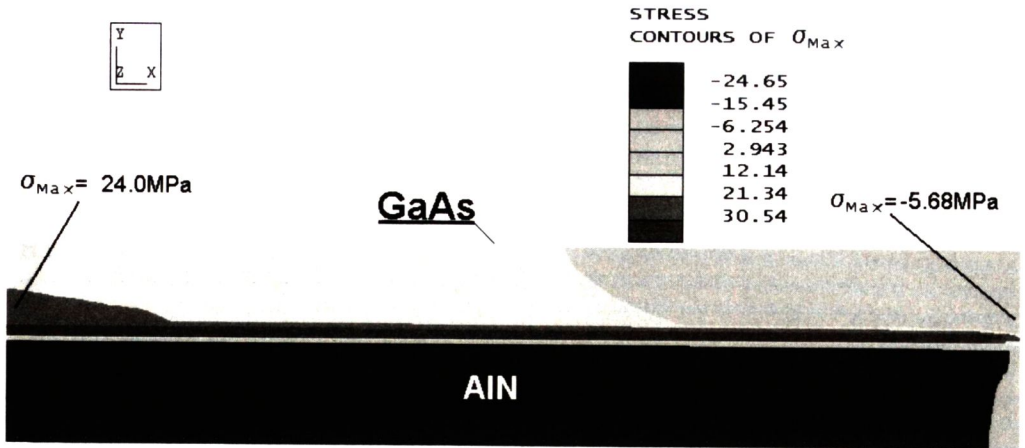


**Fig.10.** The principal residual stress distribution ( $s_{MAX}$ ) in the model bonded systems GaAs/AgCu28/AlN.

It follows from an analysis of the residual stress state in the GaAs/AlN system that the magnitude and distribution of the maximum principal stress  $\sigma_{MAX}$  in GaAs depend significantly on the axial component  $\sigma_x$  of the stress (Tab.3).

As can be seen in Fig.11, this distribution of the thermal residual stresses in the GaAs/AlN system examined is "reflected" in the final image of its deformation.

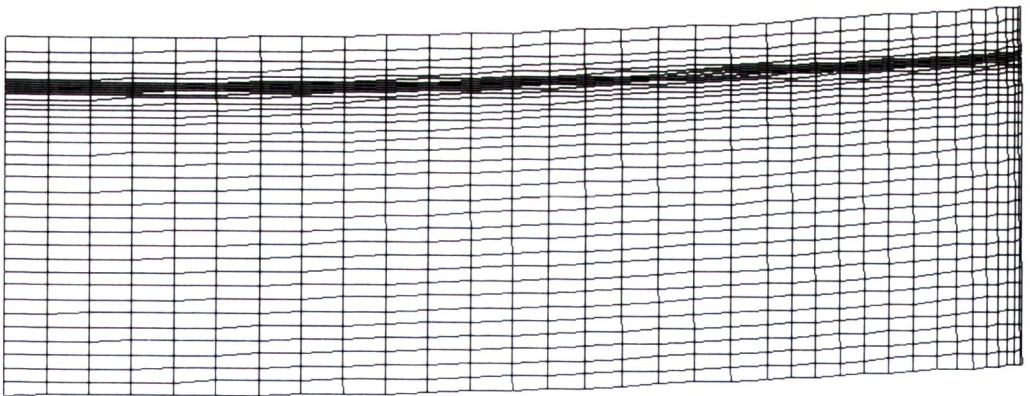


**Fig.11.** Deformation of the model GaAs/AgCu28/AlN bonded system due to a thermal load of (1003 K  $\rightarrow$  293 K).



The difference in the magnitude and distribution of the residual stresses between the GaAs/AlN system and the system with a copper or composite heatsink can be attributed to, among other things, the greater stiffness of AlN (Young modulus of AlN ceramic is  $E = 310.0$  GPa), the smaller thickness of the AlN component (0.64 mm compared to 1.8 mm with Cu or  $\text{CuC}_F$  heatsink - Fig.2), and the small difference between the thermal expansion coefficients of the two components of the GaAs/ AlN system ( $\Delta\alpha = \text{ca.} -0.7 \times 10^{-6} 1/\text{K}$ ).

#### 4. CONCLUSION

The results of our study show that:

- Heatsinks made of the  $\text{CuC}_F$  composite material ensure a considerable reduction of stresses compared to those induced in systems with conventional copper heatsinks: the maximum principal stresses  $\sigma_{\text{MAX}}$  (at the maximum stress concentration region in the GaAs) decrease about sixfold, namely, from 20 MPa (with a copper heatsink) to 3.31 MPa (with a composite heatsink). Fig.12 compares the magnitudes and distributions of the principal stress  $\sigma_{\text{MAX}}$  in the GaAs/Cu system joined using an SnPb40 solder (thermal load  $450 \rightarrow 293$  K) and an indium interlayer (thermal load  $429 \rightarrow 293$  K). It appears that with the SnPb40 solder, the maximum magnitude of the stress  $\sigma_{\text{MAX}}$  was about 4.5 times as great (15.52 MPa) as that calculated in the system with the composite heatsink even when this latter was joined using a hard AgCu28 braze (3.31 MPa). It is true that with the indium braze, the stress  $\sigma_{\text{MAX}}$  is only about 1.5 MPa, but indium has serious drawbacks as mentioned earlier (see: Introduction).

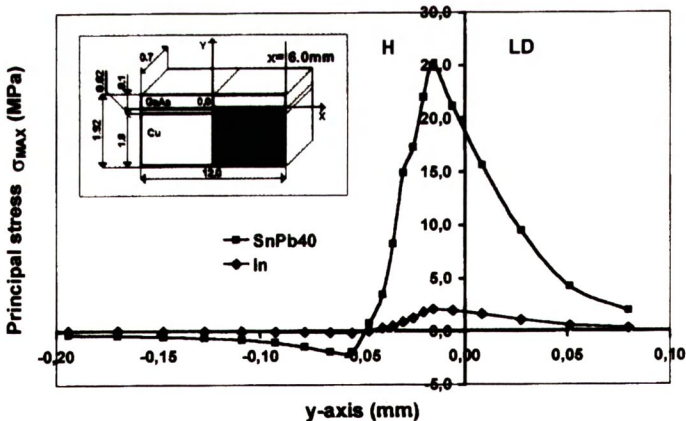


**Fig.12.** Distribution of the residual principal stress  $\sigma_{\text{MAX}}$  in the GaAs/Cu system soldered using In or the SnPb40 solder, along the y - axis ( $y \in [-0.2, 0.1]$ ) for  $x = 6.0$ , at the maximum stress concentration region.

- With the AlN ceramic heatsink, the stresses  $\sigma_{\text{MAX}}$  in the GaAs device, at its free end - near the GaAs/AlN joining line are compressive ( $\sigma_{\text{MAX}} = -5.68$  MPa). The presence of compressive stresses in this region is very beneficial, since they prevent the GaAs device from cracking, thereby increasing the mechanical strength and reliability of the entire LD/H system.

## REFERENCES

- [1] SDL Inc. (USA), 96/97 Producent Catalog, 59-61
- [2] Casey Jr H.C., Panish M.B.: *Heterostructure lasers, Part B. Materials and operating characteristics*. Academic Press, (1978)
- [3] Beach R. & co: IEEE J. Quantum Electron, 28, 4, (1992), 966-976
- [4] Periodic Progress Report: *New carbon fibre reinforced copper matrix composites for a unique and new generation of electronic and electrical devices*. CAFICOM Project, (1997)
- [5] Haybrechts F., Delanay F.: Powder Metallurgy, 34, 4, (1991), 281- 284
- [6] Blum J.B. and co.: Hybride Circuit Technology, 08, (1989), 7-14
- [7] Goldsmith A., Waterman T.E., Hirchorn H.J.: *Handbook of thermophysical properties of solid materials*. New York, (1991)
- [8] McCluskey F.P., Condra L., Torii T., Fink J.: *A materials focus*. Microelectronics International, 4, September (1996), 23-26
- [9] Blakemore J.S.: J. Appl. Ph., 53, 10, (1991), 123-181
- [10] Sadao Adachi: *Physical properties of III-V semiconductor compounds InP, InAs, GaAs, GaP, InGaAs and InGaAsP*. John Wiley & Sons, (1992)